

# Calculating the Black Hole Mass of Blazar PKS 1502+106 from Different Epochs Optical Spectra

M. Cvitan, K. Savard

Supervisors: Daryl Haggard and John Ruan

*McGill University, Montreal QC*

(Dated: July 19, 2020)

Following the [9] high-energy cosmic neutrino detection at the IceCube experiment, coincident with the flaring blazar TXS-0506+056, multimessenger astrophysics has been reinvigorated. The aim of this project is to give new and supporting evidence to neutrino-blazar links, motivated by another neutrino emission possibly originating from blazar PKS 1502+106. We are searching for changes in the optical spectrum of the blazar prior to and post neutrino detection. Using three epochs of data (two prior, one post) we use the C IV broad emission line, fitted to a Gaussian, to extract information about the blazar itself. We take steps towards using these fittings to measure the mass of the black hole powering the blazar, and do so with two independent calculations. The calculations are not consistent with each other and therefore we were unable to make any conclusions so far, but have a lot of available routes to improve our calculations.

## I. INTRODUCTION

### A. A Multimessenger Background

The recent emergence of multi-messenger astrophysics has ushered the dawn of a new era of science, where global collaborations are orchestrated across disciplines. In this regime, the classical electromagnetic observation of astrophysical sources are studied in tandem with other cosmic messengers, such as high energy neutrinos and cosmic rays in spatial and/or temporal coincidence, providing key insights into our Universe.

In this paper, we focus on neutrinos as cosmic messengers and their Electromagnetic (EM) counterparts. Since the discovery of a diffuse flux of high energy neutrinos, the only two astrophysical objects to be unambiguously identified as sources are our Sun and the supernova 1987A, at low energies [5]. The origin higher energy neutrinos remains to be determined, but is expected to be extragalactic. These same neutrinos which comprise the high-energy diffuse flux are predicted to be produced in the same (or near to) acceleration sites where cosmic neutrinos interact with matter and ambient light [8]. There have been many proposed source candidates, one of the most prominent being Active Galactic Nuclei (AGN).

AGN can be described as compact regions in the centre of a galaxy with extremely high EM luminosity over portions of the spectrum, which are distinctly non-stellar in nature. It is commonly agreed upon that the properties of AGN radiation are due to the presence of a supermassive black hole accreting matter at the centre of the host galaxy - they are by far some of the most luminous and energetic sources in the observable

universe. The radio-loud subclass of AGN includes rare blazars. Blazars constitute a class of AGN where the gravitational and/or rotational energy of the black hole is converted into collimated relativistic jets of material that are launched from the accretion flow [1]. These relativistic jets emit both gamma radiation through both synchrotron emission and inverse Compton scattering (two distinct methods of producing radiation), comprising the large majority of extragalactic gamma ray radiation seen in the sky.

Synchrotron emission is a class of radiation which does not originate from thermal processes, and instead is produced when charged particles moving at relativistic speeds spiral around magnetic field lines [1]. Due to the constant change in directions, the electrons accelerate and emit photons at energies and frequencies determined by the speed of the electron. This radiation is relativistically ‘beamed’ in a certain direction, confining it to a narrow jet perpendicular to the acceleration. Relativistic beaming causes particles moving toward the observer to appear more luminous due to a combination of relativistic and Doppler effects. Synchrotron radiation covers radio to X-ray frequencies. Inverse Compton scattering allows electrons with significant kinetic energy to transfer that energy to a photon, resulting in a higher frequency scattered photon [1]. Inverse Compton produces large amounts of gamma radiation. Blazars are particularly important as they are classified as having jets directly oriented towards Earth’s line of sight, like looking down the barrel of a gun, and therefore we observe maximal Doppler boosting.

Within the jet, particles are accelerated to high energies. Many of these particles are protons which

interact with the radiation fields and surrounding matter to produce high energy pions which will then decay into photons and neutrinos [5]. The theorized neutrino flux would therefore be directed at Earth and relativistically Doppler boosted, enhancing the observable flux.

Thanks to the enhancement in observed luminosity from Doppler boosting, blazars provide the opportunity to gain valuable insight into cosmic particle acceleration processes. In this context, neutrinos are excellent messenger particles as their only interaction with matter is via the weak force - this means they can travel across our universe virtually unimpeded by magnetic fields or interaction with other particles [8]. Should the origin of astrophysical neutrino detections be successfully linked to blazars, it would suggest that blazar jets could be the acceleration sites of ultra high energy cosmic rays, some of the most high energy particles in the universe.

On September 22nd 2017, a milestone occurred when a high-energy neutrino event was detected by the IceCube observatory, coincident in both time and direction with a gamma-ray flare emerging from a known blazar, TXS-0506+056 [6]. Follow-up searches into archival data (neutrino events and EM counterparts) revealed with 3-sigma uncertainty neutrino emission originating from the blazar direction both before and during the flare, heavily suggesting that blazars can be labelled as sources of high-energy neutrinos [7]. This general conclusion, however, still remains somewhat debated and further observations are necessary to confirm the findings.

## B. PKS 1502+106: A Possible Neutrino Origin

On 30 July 2019, at 20:50:41.31 UT IceCube detected a neutrino which was spatially coincident with another known blazar, PKS 1502+106. This blazar was previously documented in the Fermi-LAT catalogue, the only gamma-ray object lying within the 90% confidence region of the neutrino detection. Having been observed in the optical spectroscopy twice prior by the Sloan Digital Sky Survey (SDSS), the blazar was ideal for a follow-up spectroscopy, performed by the Magellan telescope (also in the optical band) on August 5th 2019. Specifically, this probes the possible factors contributing to the emission of neutrinos, by using data prior and immediately post a possible neutrino emission to look for changes in the accretion flow, which can be inferred through the optical spectra. We are approaching this project as a wide generalized search for any types of transformations in the blazar, and therefore will begin by extracting basic information (black hole mass, rate of accretion) to allow us to make further calculations.

## II. METHODS AND DATA ANALYSIS

We have three epochs of spectra available for study: two from the SDSS prior to the neutrino detection, and one from Magellan just after. We began our analysis by making a measurement of the black hole mass ( $M_{BH}$ ), a basic feature of AGN which should not change in the timescales we are concerned with ( $\approx 16$  years). In the following section we will outline the methods we used for obtaining the Black Hole Mass from the optical spectra of all three epochs. The spectra were taken as measurements of the flux density as a function of wavelength.

### A. Framework for Obtaining a Black Hole Mass

PKS 1502+106 belongs to a subclass of blazars known as Flat Spectrum Radio Quasars (FSRQ), which are characterized by their broad emission lines, featuring strong emission from Hydrogen, Helium, Carbon and Magnesium amongst others. The radiation from the accretion disk surrounding the black hole excites gravitationally bound gas in regions close to the black hole, resulting in strong emission lines at distinct wavelengths.

Aside from the emission line features, the general shape of a FSRQ at optical wavelengths assumes the form of a spectral continuum which is commonly modelled as a power law of the form

$$F_v = C v^{-\alpha} \quad (1)$$

where  $F_v$  is the flux density,  $C$  is a constant and  $\alpha$  is the power law index (typically between 0 and 1) [1]. The power law is a result of synchrotron emission from the relativistic jet dominating the continuum. If this continuum is well modelled, it can be subtracted from the spectrum allowing for detailed analysis of the emission lines.

Characteristic broadness of the emission lines themselves are due to the extremely high velocity of the gas surrounding the black hole, and results from Doppler broadening due to motion of the gas - gas moving away from the observer is Doppler shifted to longer wavelength, and gas approaching the observer is Doppler shifted to shorter wavelength, resulting in an emission line broadened in both directions.

The broadness of an emission line can be characterized by the Full-Width-Half-Max (FWHM), expressed in terms of a velocity dispersion. This can be done by fitting an emission line to a Gaussian function, modelling the ideal atomic emission lineshape with a mean centered at the predicted emission wavelength, and measuring the width (dispersion) of the spectral line at half the measured maximum flux density, derived by the

following equation:

$$FWHM = \frac{2\sqrt{2\ln(2)}\sigma}{\mu} \times c, \quad (2)$$

where  $\sigma$  is the standard deviation of a fitted peak of the Gaussian,  $\mu$  is the mean value, and  $c$  is the speed of light.

The typical approach to calculating  $M_{BH}$  is to measure the continuum luminosity ( $L_{CONT}$ ), and the FWHM of a prominent emission line, and use the following relation:

$$\log\left(\frac{M_{BH}}{M_{\odot}}\right) = a + b \log\left(\frac{L_{cont}}{10^{44} \text{ergs}^{-1}}\right) + c \log\left(\frac{FWHM}{\text{km s}^{-1}}\right), \quad (3)$$

where  $M_{\odot}$  is the mass of the sun ( $1.989 \times 10^{30} \text{kg}$ ), and the three constants  $a$ ,  $b$  and  $c$  are obtained from a linear regression analysis dependent on the emission line being measured [3]. In the case of FSRQ, the continuum luminosity is extremely difficult to measure directly from the spectrum due to it being heavily dominated by jet emission (non-thermal). However, it is possible to calculate the luminosity of the continuum through the following relation between the luminosity of the emission line ( $L_{line}$ ) and the FWHM:

$$\log\left(\frac{M_{BH}}{M_{\odot}}\right) = a + b \log\left(\frac{L_{line}}{10^{44} \text{ergs}^{-1}}\right) + 2 \log\left(\frac{FWHM}{\text{km s}^{-1}}\right), \quad (4)$$

where  $a = 0.863 \pm 0.009$  and  $b = 7.66 \pm 0.41$ , obtained from a catalog of quasar properties from the SDSS for the C IV emission line in FSRQ [3]. This relation holds because the continuum emission from the accretion disk ionizes the surrounding gas to produce broad lines. This naturally leads to a correlation between the disk continuum luminosity and the broad line luminosity. In order to calculate  $L_{line}$ , the total flux ( $F$ ) of the emission line as well as the luminosity distance of the blazar from the observer ( $D_L$ ) is needed:

$$L_{line} = 4\pi D_L^2 \quad (5)$$

Total flux is calculated by integrating under the Gaussian emission line subtracted from the continuum.  $D_L$  is calculated directly from the observed cosmological redshift of the blazar object, and assumed cosmological parameters. Assuming standard  $\Lambda$ CDM cosmology, these are equal to:  $H_0 = 70 \text{km s}^{-1}$ ,  $\Omega_M = 0.3$ ,  $\Omega_A = 0.7$ . A cosmological calculator was used to compute the value of  $D_L$  based on this cosmology [2]. Cosmological redshift can be used in this way to measure distance of astrophysical objects due to the fact that space itself is currently expanding, resulting in object to remain stationary while the distance between them increases. A sufficiently far source will have a cosmological redshift which is directly correlated to their

acceleration from earth, and this relation has been well studied by cosmologists resulting in the above equation. The effect of redshift on wavelength is described in the following equation:

$$z = \frac{\lambda_{observed} - \lambda_{rest}}{\lambda_{rest}} \quad (6)$$

where  $z$  is the redshift (a dimensionless quantity),  $\lambda_{observed}$  is the wavelength as measured in the observer frame, and  $\lambda_{rest}$  is the wavelength as measured in the rest frame. In context,  $z < 0$  describes light from objects approaching the observer, whereas  $z > 0$  describes light from objects moving away from the observer.

## B. Analysis of PKS 1502+106

For this analysis, we used the C IV emission line to measure the  $M_{BH}$  due to it's strength across all epochs of spectra. The three spectra were first cropped, such that areas with very low signal-to-noise ratios were ignored. Figure 1 shows the raw data obtained from the three epochs, plotted on a lin-log scale (the original format of the data). The C IV emission line is clearly marked.

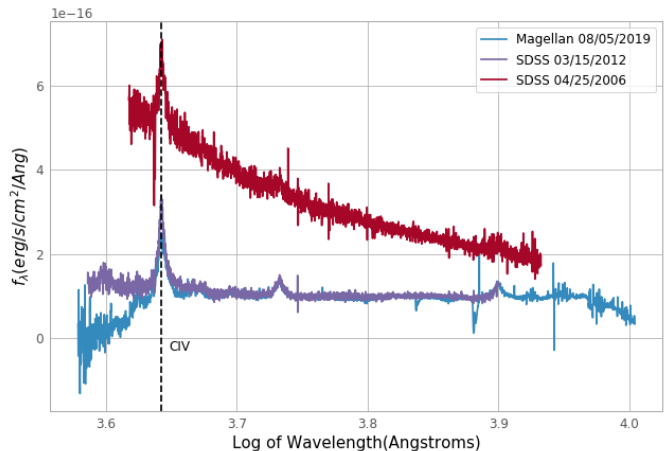


FIG. 1. Three epochs of optical spectra of the blazar PKS 1502+106. The red and purple spectra correspond to spectroscopy taken by SDSS before the detection of the neutrino, and the blue corresponds to spectroscopy performed by the Magellan telescope 5 days after the neutrino detection. C IV emission line is located with the dashed line. No redshift correction has been made on these spectra.

It is clear that the earlier of the SDSS spectrum is much more dominated by jet-emission than the other epochs, apparent by it's much higher flux density. In order to fit the underlying continuum, we first transformed the plots into log-log space. A log-log scale is necessary, as a power-law becomes linear in log space, and therefore the continuum can be fitted to a linear models. Due to the population of broad emission lines

across the continuum, it is also necessary to choose an appropriate continuum window for the fitting. There exist more robust ways to model the surrounding broad emission lines such that the continuum is not being fitted to emission regions, but for the scope of this project we decided to arbitrarily use the windows of flux on either side of the C IV emission line.

After successfully modelling the linear continuum, we returned the data to linear space and subtracted the continuum model from the C IV emission region. This process results in an emission region isolated from the continuum, resembling a Gaussian distribution:

$$f(x) = A e^{-\frac{(x-\mu)^2}{2\sigma^2}} \quad (7)$$

In order to return the data to rest-frame, a redshift correction was made to the wavelength with the measured  $z = 1.838$  from the SDSS, using Equation 6. Using a Limited Memory BFGF optimization algorithm, the data was successfully fitted to a Gaussian distribution (adjustable variables being the constant  $A$ , the mean  $\mu$ , and the standard deviation  $\sigma$ ) as is typical for emission lines.

For the purpose of this project, the data handling was done simultaneously but independently between collaborators, resulting in two processed datasets and therefore two sets of results. Not only did this ensure there was enough work to go around, but it also increased the robustness of our findings. Figures and values are distinguished with (S) and (C) to indicate which author they were produced by to enable a comparison of results.

Figures 2, 3, 4 and 5, 6, 7 show the subtracted C IV emission regions from the three epochs fitted to Gaussian distributions. This summarizes the data manipulation done in this project - all information required to calculate  $M_{BH}$  can be derived from these fits.

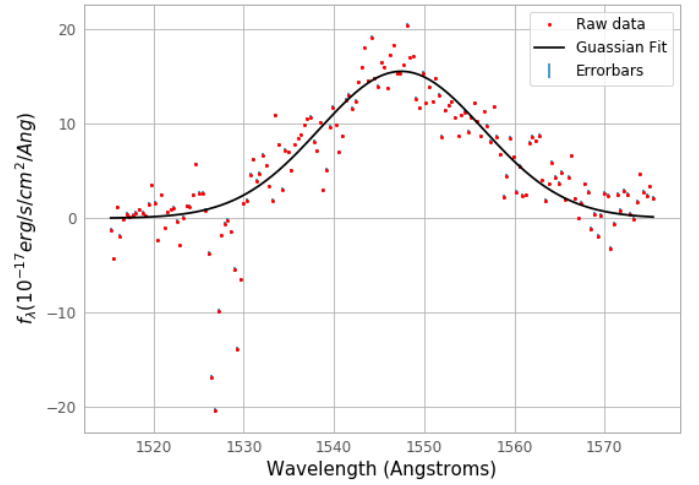


FIG. 2. The C IV emission region subtracted from the continuum, in the rest frame, from the earliest epoch of SDSS spectroscopy of the blazar PKS 1502+106 (prior to neutrino detection). The Gaussian fit resulted in the fit parameters:  $A=15.561 \times 10^{-17} \text{ erg/s/cm}^2/\text{Ang}$ ,  $\sigma = 9.085 \text{ \AA}$ ,  $\mu=1547.477 \text{ \AA}$ . (S)

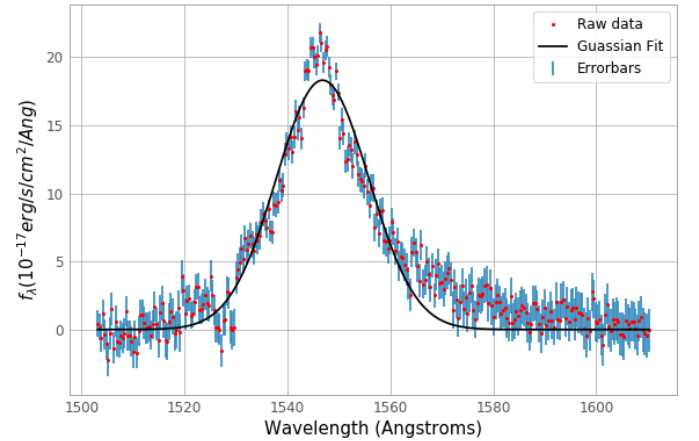


FIG. 3. The C IV emission region subtracted from the continuum, in the rest frame, from the later epoch of SDSS spectroscopy of the blazar PKS 1502+106 (prior to neutrino detection). The Gaussian fit resulted in the fit parameters:  $A=18.307 \times 10^{-17} \text{ erg/s/cm}^2/\text{Ang}$ ,  $\mu=8.990 \text{ \AA}$ ,  $\sigma=1546.827 \text{ \AA}$ . (S)

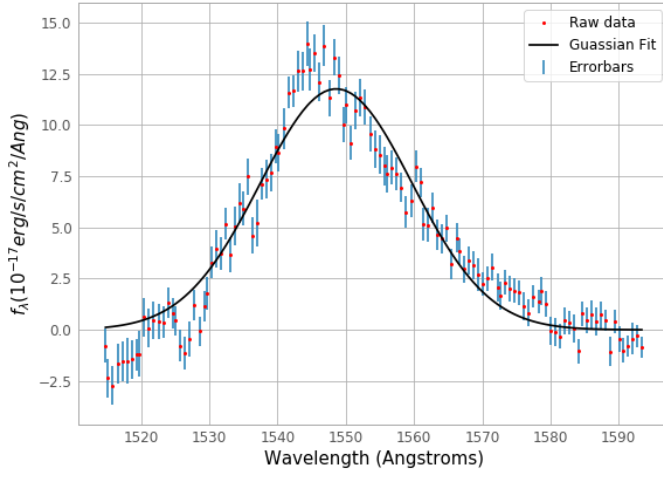


FIG. 4. The C IV emission region subtracted from the continuum, in the rest frame, from the Magellan spectroscopy of the blazar PKS 1502+106 (post neutrino detection). The Gaussian fit resulted in the fit parameters:  $A=11.769 \times 10^{-17} \text{ erg/s/cm}^2/\text{Ang}$ ,  $\mu=1548.601 \text{ \AA}$ ,  $\sigma=1548.601 \text{ \AA}$ . (S)

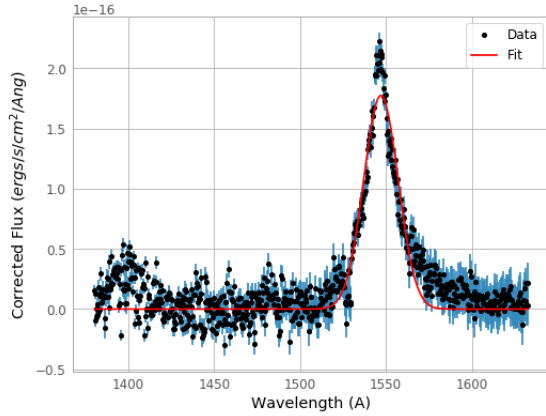


FIG. 5. A Gaussian fit performed on the C IV emission region of the data obtained from the 2012 SDSS spectrum previously outlined. The fit parameters used are a constant  $A$  of  $1.97 \times 10^{-16} \text{ erg/s/cm}^2/\text{Ang}$ , a mean of  $1574.033 \text{ \AA}$  and a standard deviation of  $10.091 \text{ \AA}$ . (C)

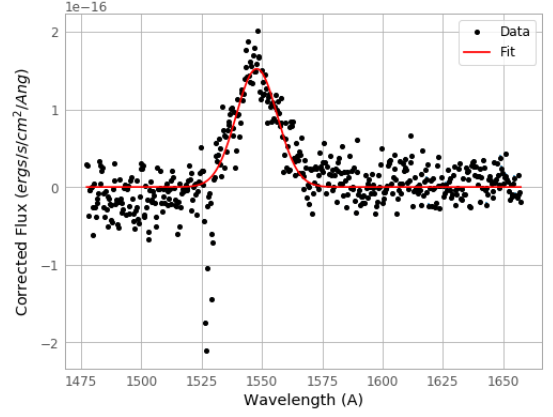


FIG. 6. A Gaussian fit performed on the C IV emission region of the data obtained from the 2006 SDSS spectrum previously outlined. The fit parameters used are a constant  $A$  of  $1.75 \times 10^{-16} \text{ erg/s/cm}^2/\text{Ang}$ , a mean of  $1547.829 \text{ \AA}$  and a standard deviation of  $8.505 \text{ \AA}$ . (C)

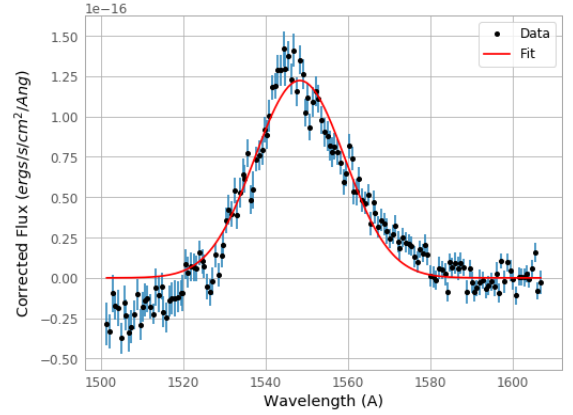


FIG. 7. A Gaussian fit performed on the C IV emission region of the data obtained from the Magellan Telescope. The fit parameters used are a constant  $A$  of  $1.52 \times 10^{-16} \text{ erg/s/cm}^2/\text{Ang}$ , a mean of  $1548.27 \text{ \AA}$  and a standard deviation of  $10.95 \text{ \AA}$ . (C)

To obtain the total flux  $F$  the Gaussian fits were integrated within a  $3\text{-}\sigma$  bound of the mean  $\mu$ . This value was then used in Equation 5 to calculate  $L_{line}$ , where  $D_L$  was calculated with the redshift  $z=1.838$  assuming  $\Lambda$ CDM cosmology and the cosmological calculator [2]. Equation 2 was used to calculate the FWHM of each dataset. With this information, we were able to calculate  $M_{BH}$  for each respective dataset independently using Equation 4.

The statistical uncertainties associated with all quantities derived from the fitting were calculated by simulating the noise in each of the spectra. It was assumed that each uncertainty associated with each data point in the spectrum was well modelled by a Gaussian distribution about the measured value. By resampling this distribution with a Monte Carlo model, we were able to repeatedly produce 'new' datasets with simulated noise. This procedure was repeated 1000 times for all three spectrum, recalculating each derived quantity for every iteration. The standard deviation of the derived quantities in the 1000 simulated datasets was taken as the statistical uncertainty associated with the quantity. The only relevant derived quantity for our purposes is  $M_{BH}$ , and they are listed in the table below:

Spectrum	$M_{BH}(\text{kg})$	$\sigma_{BH}(\text{kg})$
SDSS 2006 (S)	$1.039 \times 10^{39}$	$6.196 \times 10^{36}$
SDSS 2006 (C)	$3.081 \times 10^{38}$	$1.749 \times 10^{28}$
SDSS 2012 (S)	$1.092 \times 10^{39}$	$4.120 \times 10^{37}$
SDSS 2012 (C)	$4.952 \times 10^{38}$	$2.354 \times 10^{28}$
MAG 2019 (S)	$1.514 \times 10^{39}$	$5.781 \times 10^{37}$
MAG 2019 (C)	$5.185 \times 10^{38}$	$2.241 \times 10^{28}$

TABLE I. All calculated  $M_{BH}$  values with associated error from Monte Carlo simulation. (S) indicates it was calculated by Savard, and (C) indicates it was calculated by Cvitan.

### III. DISCUSSION

The most significant results from this analysis are the values of  $M_{BH}$  obtained. Looking at Table 1, it is clear that the two independent analyses are not in agreement. The black hole masses obtained by Savard are all about an order of magnitude larger than those obtained by Cvitan; this indicates that there are still some errors in the way that the data is being processed, and needs to be resolved in order to make a conclusive measurement of  $M_{BH}$ . Looking solely at the results of Savard, the two SDSS spectra are in agreement with each other and the Magellan spectrum is not within agreement and is slightly larger but within an order of magnitude. Cvitan also calculates a slightly larger  $M_{BH}$  (but within an order of magnitude) for the Magellan spectrum, but none of the measurements are within statistical uncertainty of each other and are therefore not in agreement. It should also be noted that Cvitan

calculates  $\sigma_{BH}$  to be up to 10 orders of magnitude smaller than the associate  $M_{BH}$  signifying a possible underestimation of statistical fluctuation.

With the current calculations, an unambiguous measurement of  $M_{BH}$  has not been achieved, and can not be until both approaches agree on a conclusion. There are factors which may have influenced the calculation of  $M_{BH}$  which may have produced varying results, such as the choice of continuum window, but should only be investigated once the magnitudes of  $\sigma_{BH}$  are resolved. It can be concluded that these results arise from faulty calculations.

It should be noted, however, that the higher mass of the Magellan spectrum was observed independently, and it could be possible that this trend will remain after the suitable correction in calculations have been made. However, the data is insufficient at this point to make conclusions.

### IV. FUTURE DIRECTIONS

The observation of any variances in the spectra is valuable, as it would further suggest that PKS 1502+106 was the source of the cosmic neutrino. If there are no significant differences detected in the spectra, it would indicate that another avenue may be necessary to study the blazar's potential to emit neutrinos.

The first challenge is to determine the source of the variations of the black hole masses; we suspect that it's simple a computational error. The arbitrary choice of continuum window and lack of proper modelling of the surrounding emission lines could also be contributing slightly to the differences in measured  $M_{BH}$ . If the errors in computation are corrected and the disparity in measurements remains, a more robust modelling of the continuum will be our first endeavour.

Once  $M_{BH}$  is successfully calculated, we will be able to extract many other meaningful values, such as the accretion rate. Observed changes in accretion rate before and after the neutrino detection gives more evidence for the blazar being the origin of the neutrino, and gives insight into the processes of neutrino emission.

It is evident that a blueshift of the C IV emission line is more prominent in the Magellan spectrum, as seen in the leftward skewing of the Gaussian form in Figures 7 and 4. It would be interesting to further study this effect and the likelihood that it is related to a high-energy neutrino emission, as this spectrum was recorded days after the PKS 1502+106 blazar flare. It is also interesting to note that the black hole mass obtained from the Magellan telescope data seems to be greater than the other two masses from the SDSS spectra for both versions of the calculation.

It is evident that there are a plethora of avenues to pursue in this project, and much work is still to be done.

## V. REFERENCES

- 
- [1] Peterson, Bradley M., An Introduction to Active Galactic Nuclei, 1997, Provided by the SAO/NASA Astrophysics Data System, 2019.
  - [2] NED Cosmology Calculator. <http://www.astro.ucla.edu/~wright/CosmoCalc.html>. 2019.
  - [3] J. J. Ruan, S. F. Anderson, R. M. Plotkin, W. N. Brandt, T. H. Burnett, A. D. Myers and D. P. Schneider. The Nature of Transition Blazars, 2014; arXiv:1410.1539. DOI: 10.1088/0004-637X/797/1/19.
  - [4] Vanden Berk, D. E., Richards, G. T., Bauer, A., et al. 2001, AJ, 122, 549
  - [5] Kohta Murase and Imre Bartos. High-Energy Multi-Messenger Transient Astrophysics, 2019, Ann.Rev.Nucl.Part.Sci. 69 (2019) 477; arXiv:1907.12506. DOI: 10.1146/annurev-nucl-101918-023510.
  - [6] A. Keivani, K. Murase, M. Petropoulou, D. B. Fox, S. B. Cenko, S. Chaty, A. Coleiro, J. J. DeLaunay, S. Dimitrakoudis, P. A. Evans, J. A. Kennea, F. E. Marshall, A. Mastichiadis, J. P. Osborne, M. Santander, A. Tohuvavohu and C. F. Turley. A Multimessenger Picture of the Flaring Blazar TXS 0506+056: implications for High-Energy Neutrino Emission and Cosmic Ray Acceleration, 2018, Astrophys.J. 864 (2018) 84; arXiv:1807.04537. DOI: 10.3847/1538-4357/aad59a.
  - [7] The IceCube, Fermi-LAT, MAGIC, AGILE, ASAS-SN, HAWC, H. E. S. S, INTEGRAL, Kanata, Kiso, Kapteyn, Liverpool telescope, Subaru, Swift/NuSTAR, VERITAS and VLA/17B-403 teams. Multi-messenger observations of a flaring blazar coincident with high-energy neutrino IceCube-170922A, 2018, Science 361, eaat1378 (2018); arXiv:1807.08816. DOI: 10.1126/science.aat1378.
  - [8] IceCube Collaboration. Neutrino emission from the direction of the blazar TXS 0506+056 prior to the IceCube-170922A alert, 2018, Science 361, 147-151 (2018); arXiv:1807.08794. DOI: 10.1126/science.aat2890.
  - [9] I. Collaboration *et al.*, Science **361**, 147 (2018)